Catalysis Today 161 (2011) 247–254

Contents lists available at ScienceDirect

Catalysis Today

journal homepage: www.elsevier.com/locate/cattod

Hydrogen peroxide automatic dosing based on dissolved oxygen concentration during solar photo-Fenton

L. Prieto-Rodríguez [a], I. Oller [a,*], A. Zapata [a], A. Agüera [b], S. Malato [a]

[a] Plataforma Solar de Almería-CIEMAT, Carretera de Senés km 4, 04200 Tabernas, Spain
[b] Pesticide Residue Research Group, University of Almería, 04120 Almeria, Spain

ARTICLE INFO

Article history:
Received 13 June 2010
Received in revised form 26 October 2010
Accepted 4 November 2010
Available online 10 December 2010

Keywords:
Advanced oxidation processes
Photocatalytic treatment
Solar photocatalysis
Wastewater decontamination

ABSTRACT

Nowadays the potential of photo-Fenton process for decontamination of biologically persistent wastewater is widely recognized. In this process, hydrogen peroxide consumption could be considered as one of the factors that considerably affects costs. This highlights that an automatically hydrogen peroxide dosing system to keep the concentration optimized throughout the process would be a valuable tool for industrial wastewater remediation plants. Automatic H_2O_2 dosing during photo-Fenton would require a precise online measuring device. Today, several expensive and unreliable in complicated wastewater hydrogen peroxide probes are commercially available. This study focuses on considering dissolved oxygen concentration (DO) as a reaction stage indicator related to H_2O_2 concentration and consumption during photo-Fenton wastewater treatment. First, specific experiments designed to find out the DO–H_2O_2 related behavior during photo-Fenton at different possible operating conditions were carried out with manual addition of H_2O_2. Afterwards, a following set of experiments was performed with automatic H_2O_2 dosing according to DO concentration maintaining this parameter between desirable set points during the photo-Fenton reaction. The obtained results demonstrated the potential for making use of the DO profile for monitoring photo-Fenton, automatically dosing H_2O_2 and determining the end point of the treatment. The active participation of oxygen in the first stages of the process by Dorfman-mechanism was confirmed.

1. Introduction

The increasing volume of wastewater poured into the environment containing non-biodegradable pollutants, pesticides, pharmaceuticals, endocrine disruptors, chlorinated hydrocarbons, etc., demands the development of powerful, clean and safe decontamination technologies. The only feasible option for such biologically persistent wastewater is the use of advanced technologies based on chemical oxidation, such as the advanced oxidation processes (AOPs).

AOPs are characterized by the production of hydroxyl radicals (•OH), the second strongest known oxidant after fluorine (2.8 V reduction potential versus standard hydrogen electrode). Due to the reactivity of hydroxyl radicals, their attack is unselective, which is useful for the treatment of wastewater containing many different pollutants [1,2]. The main drawback of AOPs is their relatively high operating costs compared to those of biological treatment [3]. Therefore, in recent years, the attention of research has been focused on AOPs that can be driven by solar radiation (photo-Fenton and heterogeneous catalysis with TiO_2), instead of using UV lamps or ozone treatments which are expensive [4–6], on the study of the influence of process parameters on the reaction rates in order to increase reactor throughput [7,8], and the analysis of toxicity and biodegradability during treatment to determine the best point for discharging wastewater or coupling with a following biological treatment [9–13]. In particular, the potential of the photo-Fenton process is widely recognized within the scientific community for its high reaction rates, its applicability with natural sunlight, and because it involves the use of non-toxic and easy-to-handle reagents [14–16].

In the photo-Fenton process, the Fenton reagent produces OH• radicals by the addition of H_2O_2 to Fe^{2+} salts. The organic pollutant degradation rate is strongly accelerated by irradiation with UV–vis light in photo-Fenton [17]. Under these conditions, the photolysis of Fe^{3+} complexes promotes Fe^{2+} regeneration and iron may be considered a true catalyst.

$$Fe^{2+} + H_2O_2 \rightarrow Fe^{3+} + OH^- + OH^\bullet \quad (1)$$

$$Fe^{3+} + H_2O + h\nu \rightarrow Fe^{2+} + H^+ + OH^\bullet \quad (2)$$

$$[Fe^{3+}L_n] + h\nu \rightarrow [Fe^{2+}L_{n-1}] + L_{ox}^\bullet \quad (3)$$

* Corresponding author. Tel.: +34 950387993; fax: +34 950365015.
E-mail address: isabel.oller@psa.es (I. Oller).

0920-5861/$ – see front matter © 2010 Elsevier B.V. All rights reserved.
doi:10.1016/j.cattod.2010.11.017

Even when sunlight is used as a source of the photons required for photo-Fenton, serious doubts about its economic feasibility for commercial applications are still harbored. In this sense, another factor considerably affecting cost is reagent consumption [18]. Hydrogen peroxide may be considered the main source of cost, as iron salts and acid (pH adjustment) are rather economical. Hydrogen peroxide can be rate-limiting if applied in concentrations that are too low. On the contrary, a very high concentration of hydrogen peroxide can compete with contaminants for the hydroxyl radicals generated and also self-decompose into oxygen and water. This highlights the role of H_2O_2 automatic dosage during a photo-Fenton treatment. In this sense, the majority of the research studies are focused on the effect of the H_2O_2 concentration on compounds degradation or on wastewater mineralization by photo-Fenton [19,20], although few studies, in which different ways of H_2O_2 dosing were evaluated, are available [21,22].

Taking into account that an optimal range of hydrogen peroxide concentration depending on the characteristics of wastewater pollution must be maintained during photo-Fenton, an automatic hydrogen peroxide dosing system to keep the concentration optimized throughout the process would be a very valuable tool for industrial wastewater remediation plants.

Hydrogen peroxide is usually measured for research and industrial activities by iodometric titration [23], spectrophotometry [24], fluorescence [25], and electrochemical methods [26]. Automatic H_2O_2 dosing during photo-Fenton would require a precise online measuring device. Today, several expensive (and unreliable in complicated wastewater or when the concentration changes rapidly, as in photo-Fenton) hydrogen peroxide probes are commercially available, e.g., an amperometric electrode (Alldos® Conex 350-2200) or the Ansell WP7 hydrogen peroxide probe, also based on a dual-electrode system. However, most hydrogen peroxide sensors currently under development or scientific study are catalase-based biosensors [27,28], which have enzyme degradation problems, or amperometric sensors [29,30], which present fouling problems and sometimes poor accuracy, possibly due to interference from dissolved oxygen. Other devices make use of direct electroanalytical determination, which is difficult, because of the quite high potentials required for oxidation of the analyte on bare electrode surfaces [31]. This analysis does therefore not seem to be realistic in a complex sample such as wastewater treated by photo-Fenton [32]. Recently, a novel strategy based on the fabrication of hydrogen peroxide non-enzymatic sensors using nanoparticles has been developed [33–35]. Although these sensors exhibit good capabilities, nanotechnology is still under study, very expensive and difficult to handle. Consequently, hydrogen peroxide automatic dosing based on these devices is not yet practicable.

These drawbacks justify the search for alternative, cheaper and more reliable assessment criteria. The relationship between dissolved oxygen (DO) concentration and hydrogen peroxide evolution during photo-Fenton could be used for this. Some authors have already studied the dependence of the mineralization rate on DO concentration throughout the photo-Fenton treatment [36,37]. In the absence of oxygen, toxic organic compounds are not completely mineralized by photo-Fenton [38]. When only traces of H_2O_2 remain in solution, DOC degradation slows down and eventually stops. At that moment, dissolved oxygen is insufficient to sustain degradation.

This study focuses on considering DO concentration as a reaction stage indicator related to H_2O_2 concentration and consumption during photo-Fenton wastewater treatment. This would allow automatic H_2O_2 dosing as a function of DO concentration measured by well-known commercial and accurate DO sensors.

A mixture of five commercial pesticides commonly used in greenhouse agriculture (Vydate, Metomur, Couraze, Ditimur-40 and Scala) has been selected as an example of polluted water for performing two different sets of photo-Fenton experiments. First, specific experiments designed to find out the DO–H_2O_2 related behavior during photo-Fenton wastewater treatment at different possible operating conditions were carried out with manual addition of H_2O_2. Afterwards, in view of these results, a following set of experiments was performed with automatic hydrogen peroxide dosing according to DO concentration in an attempt to maintain this parameter between desirable set points during the photo-Fenton reaction. In this study, there was no extra oxygen flow in the photoreactor and dissolved-oxygen-saturated wastewater was employed.

2. Materials and methods

2.1. Chemicals

Commercial formulations of Vydate® (10%, w/v, oxamyl, $C_7H_{13}N_3O_3S$), Metomur® (20%, w/v, methomyl, $C_5H_{10}N_2O_2S$), Couraze® (20%, w/v, imidacloprid, $C_{16}H_{22}ClN_3O$), Ditimur-40® (40%, w/v, dimethoate, $C_5H_{12}NO_3PS_2$) and Scala® (40%, w/v, pyrimethanil, $C_{12}H_{13}N_3$), were used as received. Distilled water used in the pilot plant was supplied by the Plataforma Solar de Almería (PSA) distillation plant (conductivity < 10 μS/cm, Cl^- = 0.2–0.3 mg/L, NO_3^- < 0.2 mg/L, organic carbon < 0.5 mg/L). Photo-Fenton experiments were performed using iron sulfate ($FeSO_4{\cdot}7H_2O$), reagent grade hydrogen peroxide (30%, w/v) and sulfuric acid for pH adjustment (around 2.6–2.8) to avoid iron salt precipitation, all provided by Panreac (analytical grade).

2.2. Analytical determinations

Mineralization was followed by measuring the dissolved organic carbon (DOC) by direct injection of filtered samples into a Shimadzu-5050A TOC analyzer with an NDIR detector and calibrated with standard solutions of potassium phthalate. Total iron concentration was monitored by colorimetric determination with 1,10-phenanthroline, according to ISO 6332, using a Unicam-2 spectrophotometer. Hydrogen peroxide concentration was analyzed in the laboratory by a spectrophotometric method using ammonium metavanadate, in which the concentration is calculated from absorption measured at 450 nm using a found by Nogueira et al. [24]. Chemical oxygen demand (COD) was measured with Merck® Spectroquant kits (ref: 1.14541.0001). The absorbance was measured with a Merck Spectroquant® NOVA 30 photometer (an external calibration curve was used).

2.3. Experimental set-up

2.3.1. Solar reactor

Photo-Fenton experiments were performed in a Compound Parabolic Collector solar pilot-plant specially developed for photo-Fenton applications and operated in batch recirculation mode. The reactor loop consists of a continuously stirred tank, a centrifugal recirculation pump (1.5 m^3/h), compound parabolic collectors and connecting tubing and valves. The solar collector is composed of four 1.04-m^2 compound parabolic collector (CPCs) units [6] (total area of 4.16 m^2), held by an aluminum profile frame mounted on a fixed platform tilted 37° and facing south. The total reactor volume is 75 L (V_T) and the total illuminated volume inside the absorber tubes is 44.6 L (V_i). The collectors were covered with aluminum sheets for mixing in the dark. The temperature inside the reactor was kept at 35 °C using a temperature control system consisting of a heating by thermal resistances in the tubing (made of stainless steel), and cooling by a heat exchanger with a secondary cooling water cycle. The steel tube is heated by 12 thermal resistances (300 W, Electrifor), which embrace the tube. Tube and resistances

are thermally insulated. A custom-designed industrial refrigerator (7 kW cooling power) supplied by KKW Riedel Kältetechnik refrigerates the water of the secondary cooling cycle (refrigeration temperature can be fixed from 5 to 35 °C). An isometric map of this photo-Fenton solar reactor is available elsewhere [39].

Temperature (PT100 sensor), pH and dissolved oxygen (DO) in the pilot plant are measured online by the corresponding WTW® Sensolyt and TriOximatic IQ system electrodes. All the online data acquisition instruments transmit their measurements by analogical outputs of their respective controllers to a series of distributed I/O modules (Advantech® ADAM 4000 series). Custom SCADA (Supervisory Control and Data Acquisition) software for this was programmed in National Instruments® Lab-VIEW 7.0 at the Plataforma Solar de Almería. This software performs data acquisition and supervisory control of the plant at the same time.

In the experiments in which hydrogen peroxide is automatically controlled as a function of dissolved oxygen, 30% (w/v) hydrogen peroxide solution was added to the batch recirculation tank by an Alldos® diaphragm dosing pump (Alldos® Primus 208 Etron Profi E26-0.8). This pump is activated by the above-mentioned SCADA software when the low set point is reached, and turned off when it reaches the high set point.

Solar ultraviolet radiation (UV) was measured by a global UV radiometer (KIPP&ZONEN, model CUV3), mounted on a platform tilted 37° (the same angle as the CPCs). This gives an idea of the energy reaching any surface in the same position with regard to the sun.

Eq. (I) was used for treatment of data acquired during the experiments, where t_n is the experimental time for each sample, UV (kJ/L) is the average solar ultraviolet radiation measured during Δt_n, A_T is the total illuminated area of collectors (m^2), V_T is the total volume of the pilot plant and $Q_{UV,n}$ is the accumulated energy (per unit of volume, kJ/L) incident on the reactor for each sample taken during the experiment:

$$Q_{UV,n} = Q_{UV,n-1} + \Delta t_n \mathrm{UV} \frac{A_T}{V_T}, \quad \Delta t_n = t_n - t_{n-1} \tag{I}$$

2.3.2. Experimental procedure

At the beginning of all the experiments, with the collectors covered and the reactor filled with 75 L of distilled water (DO in saturated conditions), the corresponding volume of each commercial pesticide was added directly to the photoreactor to attain an overall starting DOC of 200 mg/L. After at least 15 min of homogenization, a sample was taken (125 mL). Then the pH was adjusted to 2.6–2.8 with sulfuric acid. Afterwards, iron salt was also added (20 mg/L of Fe^{2+}) and well homogenized for 15 min (another sample is taken to check iron concentration). The following hydrogen peroxide addition steps were carried out depending on the type of experiment:

1. It was attempted to keep hydrogen peroxide concentration between 100 and 400 mg/L throughout the test. In this case, the original dose was 400 mg/L after the iron concentration checking sample was taken. At that moment collectors were uncovered and photo-Fenton began. Samples were taken every 15 min and H_2O_2 was measured so as consumed reagent was continuously replaced by adding between 80 and 120 mg/L of H_2O_2 to always leave excess of reagent.
2. The entire amount of H_2O_2 necessary in the first experiment for 60% of DOC elimination was added at the beginning of the process. 1200 mg/L of hydrogen peroxide were added and the collector uncovered (photo-Fenton began), samples were taken every 15 min and no more H_2O_2 was added during the test.
3. H_2O_2 was added in 80 mg/L doses as soon as the original amount was completely consumed. The first dose was added after taking the iron concentration checking sample. Then samples were taken every 10 min until H_2O_2 was completely consumed and another dose added.
4. The purpose here was to confirm the H_2O_2 to DO concentration relationship observed in the previous experiments. The original 200 mg/L of DOC were added in 40 mg/L steps. As residual DOC remained at the end of each photo-Fenton process, the DOC was always a bit higher at the beginning of the following step. Following procedure 1 for H_2O_2 dosing, once pesticides had been degraded, collectors were covered and 40 mg/L (as DOC) of pesticides were added again and homogenized with the remaining DOC. After 15 min a sample was taken and collectors uncovered again (photo-Fenton began).
5. Once the H_2O_2-to-DO ratio had been clearly defined, experiments were performed with automatically controlled hydrogen peroxide addition according to the DO. Three pairs of DO set points, 4–6, 3–5 and 1–3 mg/L, were selected considering the DO normally measured during tests. In these cases, 15 min after the addition of iron salt, a sample was taken and collectors uncovered (photo-Fenton began). Then, DO was recorded and small initial doses of hydrogen peroxide (2–20 mg/L) were added manually until DO dropped below the low set point, and the dosing pump was turned on automatically by the software. From this moment on it continued to work automatically. Samples were taken every 15 min to evaluate the photo-Fenton degradation parameters. When the high DO set point was passed the pump stopped, also automatically.

3. Results and discussion

The main parameters used to monitor the degradation and mineralization of the selected pesticides mixture were the DOC, chemical oxygen demand (COD) and the accumulated energy (Q, kJ/L) received throughout the process. Furthermore, the H_2O_2 concentration was monitored at all times (taking into account the punctual manual additions) and the amount consumed during the photo-Fenton treatment was determined. The operating conditions, were always the same, that is, original DOC of 200 mg/L, 20 mg/L of Fe^{2+}, pH 2.8–2.9 at the beginning of the experiments and temperature 35 °C. At the end of all the experiments pH achieved values not lower than 2.4 so no iron salts precipitation was observed.

Blank experiments under the same operating conditions but in absence of irradiation and in the presence or absence of the pesticides mixture under study have been previously reported by Zapata et al. [40]. In summary, it was observed that H_2O_2 consumption was noticeable higher in the presence of irradiation and the pesticide mixture. Since the regeneration of ferrous iron from ferric iron is very slow in the absence of irradiation, the reaction between ferrous ion and H_2O_2 is limited and consequently, less hydrogen peroxide is consumed. In addition, in the presence of organics, the peroxyl radical can regenerate H_2O_2, reacting with dissolved oxygen and reducing H_2O_2 consumption.

Furthermore, it is also important to evaluate the interaction of H_2O_2 with water in absence of light and organic pollutants. Polo-López et al. [41] has recently reported a hydrogen peroxide decomposition rate of 0.75 mg/L h, which is an insignificant value to take into account during a photo-Fenton experiment.

3.1. Experiment type 1: H_2O_2 kept between 100 and 400 mg/L

At the beginning of photo-Fenton, the mineralization rate was very slow (Fig. 1), and COD quickly decreased. In this stage, H_2O_2 was efficiently consumed and DO concentration decreased drastically to below 1 mg/L, demonstrating active inclusion of dissolved

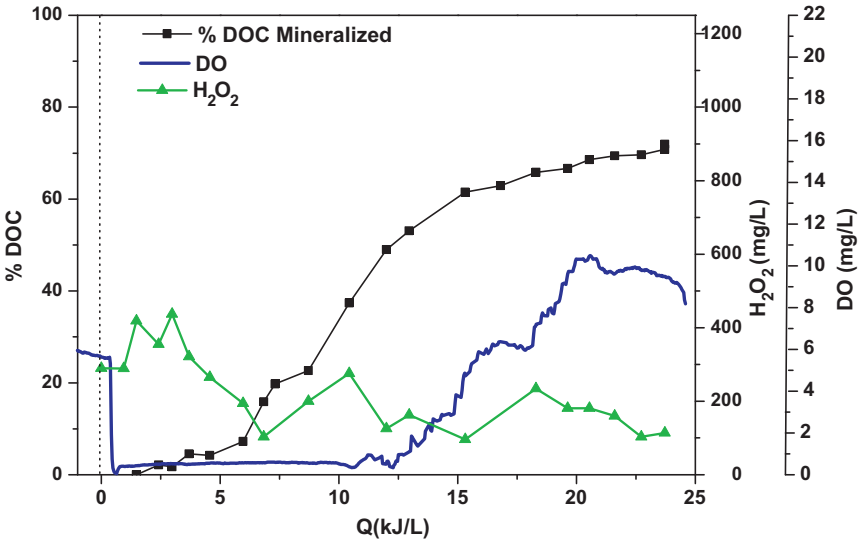

Fig. 1. Percentage of DOC mineralized, H_2O_2 and DO concentrations during photo-Fenton (Experiment type 1).

oxygen in the reaction mechanism. During the first step of the process, the reactions of OH• with organic compounds, mainly by abstracting H from R–H, N–H or O–H bonds, or adding to unsaturated bonds or to aromatic rings, lead to the formation of carbon-centered radicals. Then, carbon-centered free radicals (R•) react with dissolved oxygen following the Dorfman mechanism (reactions (4) and (5)) [42,43] and giving HO_2•, peroxyl radicals (R-O_2•) or oxyl radicals (R-O•). Decomposition of R-O_2• contributes to the oxidative degradation of organic contaminants. Peroxyl radicals eliminate hydroperoxide radical when α-substituent is an amino group as in the case of the chemical structures of the commercial pesticides used in this study [17,44].

The hydroperoxide radical (HO_2•) is also generated by reactions (6) and (7). Furthermore, the conjugate base of the HO_2• is the superoxide anion (reaction (8)), which provides another pathway for Fe^{3+} reduction to Fe^{2+} and for generation of hydroxyl radicals (reactions (9) and (10)). Hydroperoxide radicals also regenerate hydrogen peroxide by reaction (11) [17].

$$R^\bullet + O_2 \rightarrow R\text{-}O_2^\bullet \quad (4)$$

$$R\text{-}O_2^\bullet + H_2O \rightarrow ROH + HO_2^\bullet \quad (5)$$

$$Fe^{3+} + H_2O_2 \rightarrow Fe^{2+} + HO_2^\bullet + H^+ \quad (6)$$

$$OH^\bullet + H_2O_2 \rightarrow H_2O + HO_2^\bullet \quad (7)$$

$$HO_2^\bullet \Leftrightarrow O_2^{\bullet -} + H^+ \quad (8)$$

$$O_2^{\bullet -} + Fe^{3+} \Leftrightarrow O_2 + Fe^{2+} \quad (9)$$

$$O_2^{\bullet -} + H_2O_2 \rightarrow O_2 + OH^\bullet + OH^- \quad (10)$$

$$2HO_2^\bullet \Leftrightarrow H_2O_2 + O_2 \quad (11)$$

After 105 min of photo-Fenton reaction, COD strongly decreased from an original amount of 652 mg O_2/L to 254 mg O_2/L (60% removed) corresponding to only 7.26% of mineralization (Q_{UV} = 5.97 kJ/L). 2 moles of H_2O_2 are needed to mineralize 1 mol of COD, so the theoretical H_2O_2 consumption required as the oxidant reagent for this decrease in COD would be 24.9 mM, however, the real H_2O_2 consumption was 11.9 mM. This demonstrates the active involvement of dissolved oxygen in COD elimination, because there was no other oxidizing reagent in the reaction mixture as demineralized water was the test matrix.

As mentioned above, during the first steps of the process (to 10 kJ/L) the organic radical concentration (R•) was quite high and they reacted with dissolved oxygen by the Dorfman-mechanism. When mineralization rate started to increase, the concentration of "Dorfman-mechanism active radicals" dropped and hydroxyl radicals generated from H_2O_2 slowly started to react with the aliphatic compounds present at that moment in the mixture. When 60% of DOC elimination was achieved (29.5 mM of H_2O_2 consumed), the mineralization rate began to fall and H_2O_2 consumption also decreased as this reagent started to be less efficiently used by the photo-Fenton system (% DOC mineralized attained a plateau). As a result, H_2O_2 decomposition caused DO to rise to supersaturating conditions and the mineralization almost stop unless high quantities of H_2O_2 were supplied. As long as H_2O_2 addition was maintained, DO continued to rise. Nevertheless, when hydrogen peroxide addition stopped, DO returned to saturating conditions.

To summarize, DO profile has been observed to be a reaction progress indicator closely related to H_2O_2 concentration and DOC mineralization during the treatment. Furthermore, at the end of the experiment when massive oxygen production took place, hydrogen peroxide concentration increased and the mineralization rate slowed down. It is therefore important to find out whether this relationship between H_2O_2 and DO repeats when the addition of hydrogen peroxide to the photo-Fenton process is changed.

3.2. Experiment type 2: all H_2O_2 completely added at the beginning (1200 mg/L)

In this case (Fig. 2), the starting H_2O_2 concentration was higher than in experiment type 1, so DO did not fall drastically after H_2O_2 addition, but after 65 min of photo-Fenton treatment. Hydrogen peroxide concentration was so excessive that reactions (1), (3) and (6) were favored, but (12)–(14) also took place triggering generation of O_2 in the system. Therefore, the Dorfman-mechanism (reactions (3) and (4)) were important, but the consumption of DO was offset by the importance of reactions (12) and (13) at high H_2O_2 concentration, and DO decreased to below 2 mg/L only when 30% of initial H_2O_2 had been consumed. At this moment the H_2O_2 concentration was insufficient for enough DO to be generated by reactions (12)–(14). After a certain amount of mineralization, as in experiment type 1, the concentration of active "Dorfman-mechanism radicals" diminished, and therefore, the DO increased, reaching supersaturation just after 5.6 kJ/L of energy, more than twice as fast as in experiment type 1. The excess of hydrogen peroxide, compared to experiment type 1, acted as a producer of O_2 by reactions

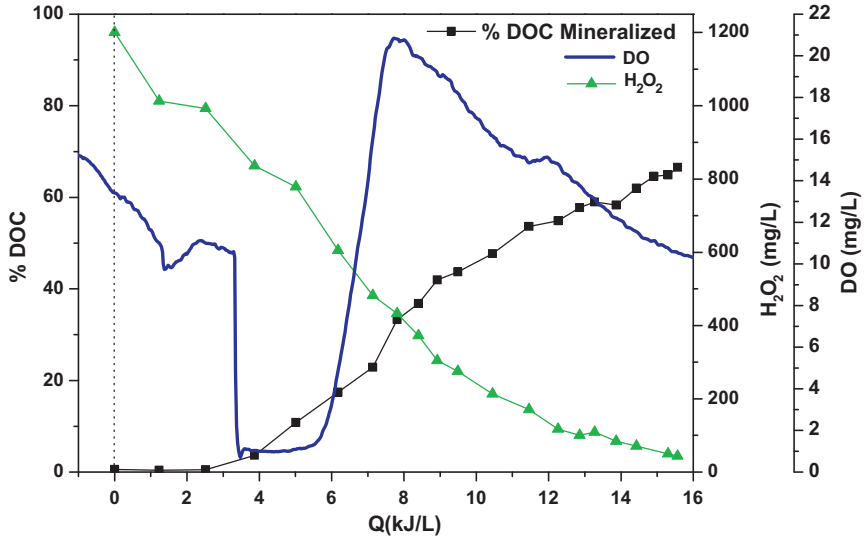

Fig. 2. Percentage of DOC mineralized, H_2O_2 and DO concentrations during photo-Fenton (Experiment type 2).

(12) and (13).

$$2H_2O_2 \Leftrightarrow O_2 + 2H_2O \quad (12)$$

$$Fe^{3+} + H_2O_2 \Leftrightarrow Fe^{2+} + O_2 + 2H_2O \quad (13)$$

$$Fe^{3+} + HO_2^{\bullet} \Leftrightarrow Fe^{2+} + O_2 + H^+ \quad (14)$$

In this experiment, H_2O_2 efficiency in producing hydroxyl radicals was very low from the first stages of the photo-Fenton treatment. This is demonstrated by the fact that 50% of COD elimination (from 623.0 mg/L to 310.2 mg/L) occurred only after 12 kJ/L at which moment almost 60% of mineralization was also attained (33.2 mM of H_2O_2 consumed). Therefore, the theoretical amount of H_2O_2 required would be 20 mM while the real H_2O_2 consumption was much higher, 30.3 mM. In experiment type 1, 652 mg O_2/L to 254 mg O_2/L (60% COD removed) corresponded to only 7.26% of mineralization and 5.97 kJ/L. Comparing COD degradation in experiments types 1 and 2, 11.9 mM and 30.3 mM of H_2O_2 were need, respectively. This highlights how inefficient is the consumption of H_2O_2 when the entire oxidizing reagent needed for wastewater mineralization is added in one step at the beginning of the treatment. During the final step of the experiment, the effect was the same as in experiment type 1. When the hydrogen peroxide concentration was depleted, the DO concentration decreased to saturation.

Operating conditions in experiment types 1 and 2 are those normally used in photo-Fenton applications, so the intermediate situation in H_2O_2 dosing would be manual addition in steps, which corresponds to experiment type 3.

3.3. Experiment type 3: H_2O_2 added in steps after total consumption (80 mg/L each time)

In this case, 160 mg/L of H_2O_2 were added at the beginning, although only 80 mg/L were added manually in the following steps after the original amount had been completely consumed (Fig. 3). The DO profile observed in each step is quite similar to the one found in experiment type 1. That is, immediately after H_2O_2 was added, DO decreased drastically to 2 mg/L (active participation of reactions (4) and (5)) and began to increase to saturation as H_2O_2 was consumed. At low H_2O_2 concentrations, R• were not produced and therefore reactions (4) and (5) were not viable and reaction (1) did not produce Fe^{3+}. When H_2O_2 (80 mg/L) was added again, the mineralization rate began to rise and DO was depleted. H_2O_2 started to be less efficiently used and DO rose with higher accumulated energy. Afterwards, DO concentration rose continuously until, at the end of the process (60% mineralization), supersaturation (12 mg/L) was reached.

It is important to highlight that when 60% mineralization was attained, 56% of COD had already been eliminated (from 601.7 mg/L to 264.7 mg/L at Q_{UV} = 34 kJ/L) which corresponds to a theoretical H_2O_2 consumption of 21.1 mM, while the real amount of H_2O_2 consumed was 16.9 mM. This is because of the small amount of H_2O_2 added at the beginning of the experiment which led to more efficient usage of this reagent and inhibited reactions (7), (12) and (13).

Summarizing, when COD was eliminated quickly, the limited concentration of H_2O_2 added was efficiently used in photo-Fenton reactions so no H_2O_2 decomposition or scavenger reactions with hydroxyl radicals occurred. Furthermore, reactions (4) and (5) were unimportant. At the end of the process, when DOC almost reached a plateau, H_2O_2 added was used inefficiently and reactions (12) and (13) triggered strong generation of DO.

Experiment types 1 and 2 were quite similar with regard to accumulated energy (around 14 kJ/L) and total H_2O_2 consumption (around 35 mM) required for 60% mineralization. Nevertheless, H_2O_2 consumption was much lower in experiment type 3 (around 17 mM for 60% mineralization) although much more accumulated energy and longer processing time was needed. This demonstrates how when H_2O_2 is added in steps (as in experiment type 3) it is used more efficiently during the photo-Fenton treatment.

3.4. Experiment type 4: treating 200 mg/L of total DOC in five steps (40 mg/L DOC)

This fourth set of experiments (Fig. 4) was designed to confirm the H_2O_2-DO relation observed in previous experiments by using a lower initial DOC concentration than 200 mg/L, which was added in four steps (40 mg/L each). DO was only monitored during the five photo-Fenton experiments and not during the transition periods in which the pesticides mixture (40 mg/L of DOC) were added and no oxidation was performed. The DO profile showed the same behavior observed in previous tests in every step of the way. When photo-Fenton treatment started and H_2O_2 concentration was high, DO decreased. When the mineralization rate slowed down, DO became supersaturated. In this case, as the organic load in each cycle was much lower than in previous experiments, higher

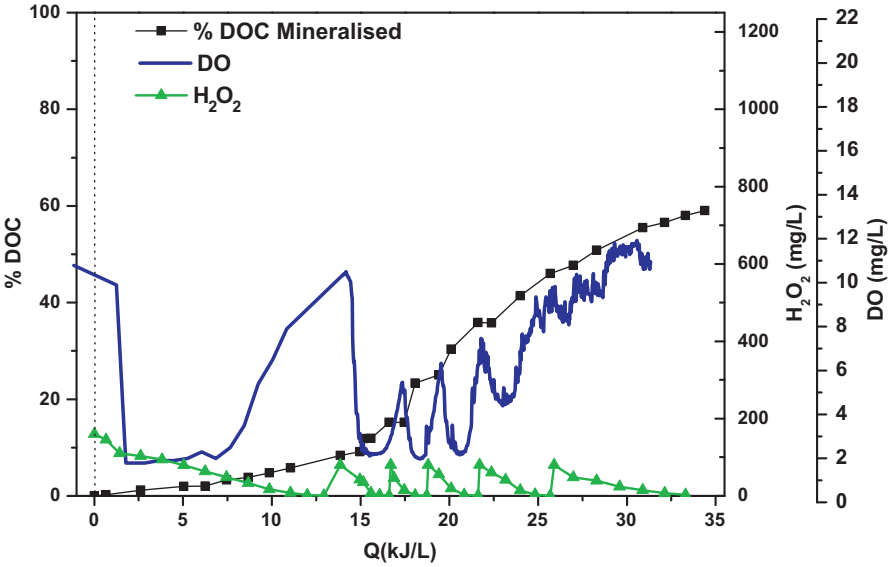

Fig. 3. Percentage of DOC mineralized, H_2O_2 and DO concentrations during photo-Fenton (Experiment type 3).

amounts of H_2O_2 were inefficiently consumed, and DO reached supersaturation more easily. Consequently, at the end of the experiment, although DOC mineralization was similar, H_2O_2 total consumption and energy were much higher than in the previous experiments.

Finally, it is important to highlight that all the experiments have been performed with H_2O_2 concentrations lower than 400 mg/L so there was not enough excess of hydrogen peroxide to provoke the auto-scavenger effect trapping hydroxyl radicals generated (reaction (7)). Only in the second type of experiment, in which all the necessary amount of H_2O_2 was added at the beginning of the process, the concentration of this reagent was 1400 mg/L but the auto-scavenger effect was not observed as the mineralization rate remained constant while H_2O_2 concentration decreased from 800 mg/L to 50 mg/L.

The auto-scavenger effect of H_2O_2 trapping generated hydroxyl radicals will be also avoided when automatic dosing of this reagent is carried out.

3.5. *Automatic dosing of H_2O_2*

From the four types of experiments in which H_2O_2 was added manually under all possible operating conditions, it may be concluded that H_2O_2 and DO profiles are inherently related during the photo-Fenton treatment of wastewater. Summarizing, at the beginning of the process, when COD was being rapidly degraded (high consumption of O_2), DO concentration dropped to below 2 mg/L. Then, as long as the mineralization rate remained high; H_2O_2 was efficiently used and the DO concentration remained low. However, the moment the mineralization reaction slowed down, H_2O_2 was

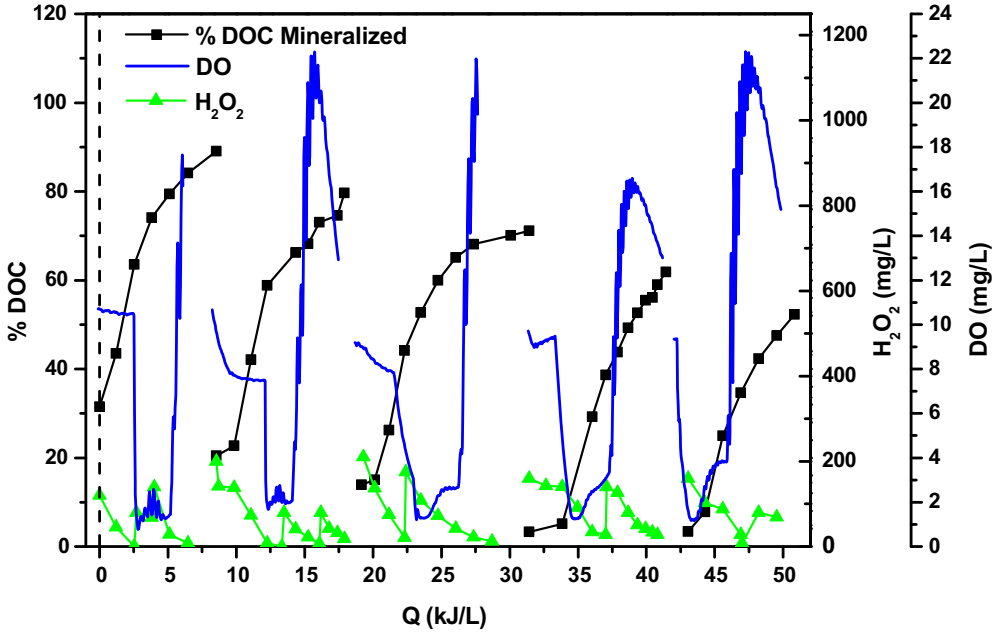

Fig. 4. Percentage of DOC mineralized, H_2O_2 and DO concentrations during photo-Fenton (Experiment type 4).

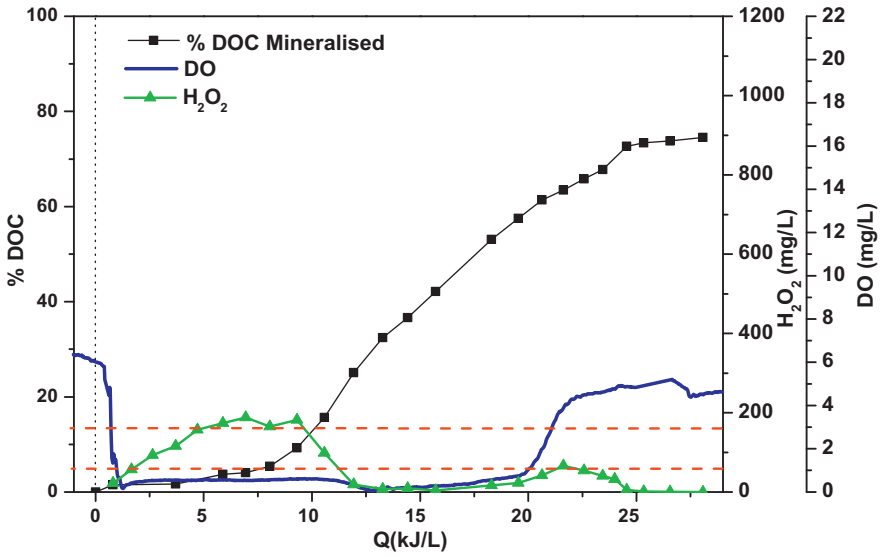

Fig. 5. Percentage of DOC mineralized, H_2O_2 and DO concentrations during photo-Fenton (DO set points at 1–3 mg/L, dashed line).

inefficiently consumed and DO generated was not consumed. Right at the end of the treatment, when the mineralization rate was very low, and H_2O_2 was being consumed slowly, the system reached supersaturation. These findings could therefore be used to manage automatic H_2O_2 dosing. Based on certain DO set points, photo-Fenton treatment could be optimized to H_2O_2 consumption. As no experience with the automatic dosing of H_2O_2 by DO probe measurements were known, it was decided to test three different cases in which the DO set points for turning automatically the H_2O_2 peristaltic pump on and off were varied. It was always necessary to add an initial small amount of H_2O_2 (between 2 and 20 mg/L) to start photo-Fenton and decrease DO which was saturated at the beginning of the treatment. This again demonstrated that reactions (9) and (10) did not participate at the first photo-Fenton stages. Reactions (4) and (5) did, but only at the beginning with the first $R^{\bullet}$.

DO automatic control set points tested were 4–6 mg/L, 3–5 mg/L and 1–3 mg/L and the flow rate was 4 mg/L min of H_2O_2. When DO was set between 4 and 6 mg/L, it decreased below 2 mg/L and when automatic dosing turned off at 6 mg/L, DO became supersaturated and H_2O_2 accumulated in water without being used in the process. At 3–5 mg/L DO behavior was quite similar but with less accumulation of H_2O_2.

Finally, at set points of 1–3 mg/L (Fig. 5), DO was below 1 mg/L for almost the same experimental time as in previous tests and 60% mineralization was attained with the same accumulated energy as in experiment types 1 and 2. Total H_2O_2 consumption was 32 mM for 60% mineralization. The main advantage observed in Fig. 5 was a higher H_2O_2 accumulation at the beginning necessary for rapid mineralization afterwards and less accumulation when the mineralization rate slowed down. 50% COD was removed in the first stage of the process up to 8 kJ/L; with H_2O_2 consumption of around 10 mM while the theoretical amount calculated was around 20 mM. The main disadvantage was the extremely low concentration of H_2O_2 when the mineralization rate was at the maximum. This effect provoked the reaction slowed down and the necessity of higher accumulated energy for attaining 60% of mineralization. An optimized H_2O_2 automatic dosing would avoid this sharp drop in H_2O_2 concentration and higher mineralization rates would be attained with lower accumulated energy.

The crucial point was at the end of the process, when DOC mineralization was 60% and residual H_2O_2 concentration was so low, which is important for later disposal of the treated wastewater into a biological treatment.

4. Conclusions

Results confirmed the inherent relationship between H_2O_2 and DO during photo-Fenton treatment. Therefore, the potential for making use of the DO profile for monitoring photo-Fenton, automatically dosing H_2O_2 and determining the end point of the treatment is demonstrated. The importance of the Dorfman-mechanism during the first stages of the process when certain radicals are present, and in consequence, the active participation of oxygen, has been shown. Optimization of automatic dosing to avoid the final drop in H_2O_2 when mineralization rates are high is still pending. Another important matter would be direct oxygen injection into the photoreactor to maximize the Dorfman-mechanism (and minimize H_2O_2 consumption) at the beginning of the process. Finally, it would be necessary to check the feasibility of DO sensors application for automatically control the hydrogen peroxide dosing during the photo-Fenton treatment of different types of real wastewater.

Acknowledgements

The authors wish to thank the Spanish Ministry of Science and Innovation for financial support under EDARSOL project (reference: CTQ2009-13459-C05-01). They also wish to thank Mrs. Deborah Fuldauer for English language correction. Lucía Prieto-Rodríguez would like to thank the University of Almeria and CIEMAT-PSA for her Ph.D. research grant.

References

[1] P.R. Gogate, A.B. Pandit, Adv. Environ. Res. 8 (2004) 501–551.
[2] M. Pera-Titus, V. García-Molina, M.A. Baños, J. Giménez, S. Esplugas, Appl. Catal. B: Environ. 47 (2004) 219–256.
[3] C. Comninellis, A. Kapalka, S. Malato, S.A. Parsons, I. Poulios, D. Mantzavinos, J. Chem. Technol. Biotechnol. 83 (2008) 769–776.
[4] J.M. Herrmann, Top. Catal. 14 (2005) 48–56.
[5] R.J. Braham, A.T. Harris, Ind. Eng. Chem. Res. 48 (2009) 8890–8905.
[6] S. Malato, P. Fernández-Ibáñez, M.I. Maldonado, J. Blanco, W. Gernjak, Catal. Today 147 (2009) 1–59.
[7] A. Zapata, I. Oller, E. Bizani, J.A. Sánchez-Pérez, M.I. Maldonado, S. Malato, Catal. Today 144 (2009) 94–99.

[8] F. Ay, E.C. Catalkaya, F. Kargi, J. Hazard. Mater. 162 (2009) 230–236.
[9] M. Bressan, L. Liberatorre, N.D. Alessandro, L. Tonucci, C. Belli, G. Ranalli, J. Agric. Food Chem. 52 (2004) 1228–1233.
[10] V. Sarria, S. Parra, N. Adler, P. Péringer, N. Benitez, C. Pulgarin, Catal. Today 76 (2002) 301–315.
[11] D. Mantzavinos, E. Psillakis, J. Chem. Technol. Biotechnol. 79 (2004) 431–454.
[12] O. Gonzalez, C. Sans, S. Esplugas, J. Hazard. Mater. 146 (2007) 459–464.
[13] V. Sarria, S. Kenfack, O. Guillod, C. Pulgarín, J. Photochem. Photobiol. A: Chem. 159 (2003) 89–99.
[14] R. Liu, H.M. Chiu, C.-S. Shiau, R.Y-L. Yeh, Y.-T. Hung, Dyes Pigments 73 (2007) 1–6.
[15] F. Torrades, J. García-Montaño, J.A. García-Hortal, X. Doménech, J. Peral, Sol. Energy 77 (2004) 573–581.
[16] R. Bauer, G. Waldner, H. Fallmann, S. Hager, M. Klare, T. Krutzler, S. Malato, P. Maletzky, Catal. Today 53 (1999) 131–144.
[17] J.J. Pignatello, E. Oliveros, A. MacKay, Crit. Rev. Environ. Sci. Technol. 36 (2006) 1–84.
[18] I. Muñoz, J. Peral, J.A. Ayllón, S. Malato, M.J. Martin, J.-Y. Perrot, M. Vincent, X. Domènech, Environ. Eng. Sci. 24 (2007) 638–651.
[19] H. Fallmann, T. Krutzler, R. Bauer, S. Malato, J. Blanco, Catal. Today 54 (1999) 309–319.
[20] M.I. Pariente, F. Martínez, J.A. Melero, J.A. Botas, T. Velegraki, N. Xekoukoulotakis, D. Mantzavinos, Appl. Catal. B: Environ. 85 (2008) 24–32.
[21] H.I. Nilsun, Water Res. 33 (1999) 1080–1084.
[22] I. Oller, S. Malato, J.A. Sánchez-Pérez, M.I. Maldonado, W. Gernjak, L.A. Pérez-Estrada, J.A. Muñoz, C. Ramos, C. Pulgarín, Ind. Eng. Chem. Res. 46 (2007) 7467–7475.
[23] W. Gernjak, T. Krutzler, A. Glaser, S. Malato, J. Caceres, R. Bauer, A.R. Fernández-Alba, Chemosphere 50 (2003) 71–78.
[24] R.F.P. Nogueira, M.C. Oliveira, W.C. Paterlini, Talanta 66 (2005) 86–91.
[25] A. Gomes, E. Fernandes, J.L.F.C. Lima, J. Biochem. Biophys. Methods 65 (2005) 45–80.
[26] F. Ricci, G. Palleschi, Biosens. Bioelectron. 21 (2005) 389–407.
[27] K.B. O'Brian, S.J. Killoran, R.D. O'Neill, J.P. Lowry, Biosens. Bioelectron. 22 (2007) 2994–3000.
[28] A.J. Guwy, F.R. Hawkes, S.R. Martin, D.L. Hawkes, P. Cunnah, Water Res. 34 (2000) 2191–2198.
[29] P. Westbroek, E. Temmerman, P. Kiekens, Anal. Chim. Acta 385 (1999) 423–428.
[30] A. Mehta, S. Patil, H. Bang, H.J. Cho, S. Seal, Sens. Actuator A 134 (2007) 146–151.
[31] G.G. Guilbault, G.J. Lubrano, Anal. Chim. Acta 64 (1973) 439–455.
[32] M. Oliveira Salles, T.R.L.C. Paixão, M. Bertotti, Int. J. Electrochem. Sci. 2 (2007) 248–256.
[33] W. Zhao, H. Wang, X. Qin, X. Wang, Z. Zhao, Z. Miao, L. Chen, M. Shan, Y. Fang, Q. Chen, Talanta 80 (2009) 1029–1033.
[34] X. Bo, J. Bai, L. Wang, L. Guo, Talanta 81 (2010) 339–345.
[35] A. Gutes, I. Laboriante, C. Carraro, R. Maboudian, Sens. Actuator B: Chem. 147 (2010) 681–686.
[36] B. Utset, J. Garcia, J. Casado, X. Domenech, J. Peral, Chemosphere 41 (2000) 1187–1192.
[37] J.M. Monteagudo, A. Durán, I. San Martin, M. Aguirre, Appl. Catal. B: Environ. 89 (2009) 510–518.
[38] C.A. Tolman, D.H.R. Barton, The Activation of Dioxygen and Homogeneous Catalytic Oxidation, Plenum Press, New York, 1993.
[39] M.I. Maldonado, P.C. Passarinho, I. Oller, W. Gernjak, P. Fernández, J. Blanco, S. Malato, J. Photochem. Photobiol. A: Chem. 185 (2007) 354–363.
[40] A. Zapata, I. Oller, L. Rizzo, S. Hilgert, M.I. Maldonado, J.A. Sánchez-Pérez, S. Malato, Appl. Catal. B: Environ. 97 (2010) 292–298.
[41] M.I. Polo-López, I. García-Fernández, I. Oller, P. Fernández-Ibáñez, Photochem. Photobiol. Sci., doi:10.1039/c0pp00174k.
[42] L.M. Dorfman, I.A. Taub, R.E. Bühler, J. Chem. Phys. 36 (1962) 3051–3061.
[43] C. Von Sonntag, P. Dowideit, X. Fang, R. Mertens, X. Pan, M.N. Schuchmann, H.-P. Schuchmann, Water Sci. Technol. 35 (1997) 9–15.
[44] C. Von Sonntag, H.P. Schuchmann, Angew. Chem. Int. Ed. Engl. 30 (1991) 1229–1253.